

# Post annealing effect on structural and optical properties of ZnO thin films derived by sol–gel route

Amanpal Singh · Dinesh Kumar · P. K. Khanna ·  
Mukesh Kumar · B. Prasad

Received: 11 June 2013 / Accepted: 13 August 2013 / Published online: 25 August 2013  
© Springer Science+Business Media New York 2013

**Abstract** Zinc oxide thin films have been spun coated on p-Si (100) substrates by sol–gel route. These films were annealed at different annealing temperatures from 300 to 1,000 °C in the oxygen ambient. In this way a suitable annealing temperature window for the sol–gel derived ZnO films exhibiting minimum defects (points and dislocations) and better quality (crystal and optical) was investigated. The structural and optical features of ZnO thin films have been examined by X-ray diffraction, atomic force microscopy, UV–Vis spectroscopy, and photoluminescence spectra. The results revealed that the crystallization in the films initiated at 300 °C, improved further with annealing. All the deposited films exhibited wurtzite phase with c-axis orientations. The variations in the position of characteristic (002) peak, stress, strain and lattice parameters are investigated as a function of annealing temperature. The optical band gap is not significantly affected with annealing as observed by UV–Vis transmission spectroscopy. The Photoluminescence spectra exhibited three luminescence centers. The near band edge emission was observed in UV region which enhanced with the heat treatment, is an indication of improvement in the optical quality of films. The other two visible emissions are related to native defects in ZnO lattice were appeared only for higher annealing ( $\geq 700$  °C).

## 1 Introduction

With a direct band gap of 3.37 eV [1] and a large exciton binding energy of 60 meV at room temperature [1, 2], ZnO is one of the most attractive candidates for a host of optical devices such as light emitting diodes [3, 4], blue and UV lasers [5], UV detectors [6] due to its potential of high operating efficiency at high temperatures. A lot of attention has been paid to the fabrication of the high quality ZnO thin films. Pulsed laser deposition (PLD) [7], rf and reactive dc sputtering [8, 9], metalorganic chemical vapor deposition (MOCVD) [10], molecular beam epitaxy (MBE) [11] are preferred methods to achieve high quality ZnO thin films. Apart from these expensive, complicated and time consuming routes, the sol–gel process is an attractive method for deposition of ZnO thin films since it has advantages of easy compositional modifications, simple and inexpensive equipment, excellent control on stoichiometry, simple in process and easy properties modulation by doping [12]. The effect of annealing temperature on structural and electrical properties significantly depends on the film deposition method. Sputtered ZnO films are shown with improvement in film quality [13], while e-beam and PLD grown films observed with enhancing the defects in crystal lattice [14] as the annealing temperature was increased above 400 °C.

In this work, ZnO thin films were deposited on p-Si (100) substrates with spin coating sol–gel route. The films were annealed at different temperatures from 300 to 1,000 °C. The effect of post annealing on the structural, optical and electrical properties of ZnO thin film such as stress, strain, grain size, transmittance, optical band gap, photoluminescence, carrier concentrations, hall mobility and resistivity are presented. Also attempts are made to find optimized annealing temperature for sol–gel derived ZnO films with minimum

A. Singh (✉) · D. Kumar · M. Kumar · B. Prasad  
Department of Electronic Science, Kurukshetra University,  
Kurukshetra, India  
e-mail: amanbkn@gmail.com

A. Singh · P. K. Khanna  
CSIR-Central Electronics and Engineering Research Institute,  
Pilani, India

defects (point and dislocations) which could be beneficial for device fabrication using the ZnO films.

## 2 Experimental

ZnO thin films were deposited on p-Si (100) and quartz substrates via sol–gel spin coating method. As a starting material zinc acetate dihydrate [ $\text{Zn}(\text{CH}_3\text{COO})_2 \cdot 2\text{H}_2\text{O}$ , 99.5 % purity] was used as a zinc source. 2-methoxy ethanol [ $\text{CH}_3\text{OCH}_2\text{CH}_2\text{OH}$ , 99.5 % purity] and ethanolamine [ $\text{C}_2\text{H}_7\text{NO}$ , 99.5 % purity] were used as a solvent and stabilizer respectively. The concentration of this solution was maintained at 0.2 mol/l. The molar ratio of ethanolamine to zinc acetate was preserved at 2:1. This solution was kept on continuous stirring for 1 h then filtered by Whatman's grade GFA glass microfiber filter papers. The obtained sol was transparent, clear, homogeneous and stable at room temperature. P-Si wafers were ultra-cleaned through the standard Radio Corporation of America (RCA) cleaning process. After aging the stable solution up to 48 h for necessary hydrolysis process [15], the solutions were spun coated on the substrates. The coating sol was dropped on the substrate which was rotated at 3000 RPM for 1 min and dried by blowing hot air during the last few seconds of spinning, so that films can be prevented from cracks due to surface tension contraction. Each layer was baked at 280 °C with the help of hot plate for 1 min. This procedure from coating to baking of the film was repeated several times to obtain multilayered film with a workable thickness. The thickness of the film was maintained around 100 nm as measured by surface profiler. This sample was cut in eight equal pieces and these samples were annealed at different temperatures 300 to 1,000 °C in the oxygen ambient for an hour in a tube furnace.

The crystal phase structure was analyzed with a XPERT-PRO diffractometer from Panalytical, equipped by a Giono-meter PW3050/60 working with Cu  $K\alpha$  radiation of wavelength  $\lambda = 1.54060 \text{ \AA}$ . Rocking curves were carried out using Bruker D8 High resolution X-ray diffraction machine. The microstructure was analyzed by atomic force microscope (AFM); model Pro 47, NT MDT. The optical transmittance spectra were observed with the help of Perkin–Elmer lambda-650 UV–VIS spectrophotometer. The photoluminescence (PL) measurements were carried out by RPM 2000 photoluminescence mapper equipped with Nd-YAG laser employing an excitation wavelength of 266 nm.

## 3 Results and discussion

Figure 1 show X-ray diffraction (XRD) spectra of ZnO thin films which were annealed at different temperatures

from 300 to 1,000 °C. The predomination of (002) peak in the observed patterns proved that the ZnO films were deposited with wurtzite crystallinity and preferential orientation was noticed along the  $c$  axis. With the increase of post annealing temperature, a dominant raise of XRD intensity revealed that the crystallinity of ZnO films was improved significantly with increasing the annealing temperature. The intensity of (002) diffraction peaks for sample annealed at 600 °C and 700 °C is observed almost six times higher than the samples annealed at 800 and 900 °C and it was almost forty times higher compared to the samples annealed at 300 and 400 °C. Fujimura et al. [16] suggested that the surface energy density of the (002) orientation was the lowest in the ZnO crystal. At high temperatures, the atoms have sufficient diffusion activation energy to occupy the correct site in the crystal lattice, and grains with lower surface energy will become larger. The growth orientation develops in the crystallographic direction of low surface energy, leading to improved ZnO crystallinity. It was observed that for the samples annealed at 1,000 °C, the intensity of XRD characteristic peak (002) extensively reduced may be due to breakage of bonds and/or reaction with substrate and/or creation of  $\text{SiO}_2$  layer at the interface. At lower annealing temperatures, peaks related to other planes (100) and (101) of the wurtzite structure were appeared to be visible but these peaks get lowered with annealing, it is indicating to reduction in the polycrystalline nature of the films. A monotonically decrease in the full width at half maxima (FWHM) of (002) peak with the annealing has been observed, which attributed to increase in the size of crystallites. Lattice parameter ' $c$ ' and ' $a$ ' were calculated by using  $c = \frac{\lambda}{\sin \theta}$  and  $a = \frac{\lambda}{\sqrt{3} \sin \theta}$  from (002) and (100) peaks respectively [17] and reproduced in Table 1. The (002) peak shifted towards higher angle from  $34.699^\circ$  to  $34.723^\circ$  with annealing from 300 to 900 °C respectively. The shifting of (002) peak toward higher angle attributed to better crystallinity with more relaxation due to annealing [18]. The average grain sizes were calculated by Scherer formula [19]

$$D = \frac{0.9\lambda}{\beta \sin \theta}$$

where  $\beta$  is the FWHM in radians,  $\lambda$  is the wavelength of Cu  $K\alpha$  radiation and  $\theta$  is Bragg's diffraction angle. As expected, the average crystallite size was increased with annealing from 15.58 nm (300 °C) to 38.97 nm (1,000 °C).

Stress in the deposited thin films is possibly due to the differences in thermal expansion coefficients and/or from the microstructure of the films. The biaxial stress ( $\epsilon_{zz}$ ) in the films can be calculated by following expression [19, 20]

$$\epsilon_{zz} = -233 \left( \frac{c_{film} - c_{bulk}}{c_{bulk}} \right) GPa$$

$c_{bulk}$ ,  $c_{film}$  are the lattice constants of standard ZnO powder ( $c_{bulk} = 5.205 \text{ nm}$ ) and deposited films respectively. Evaluated stress for ZnO films annealed at different temperature is given in Table 1. The positive and non-zero values specified that the films are deposited under the state of compressive type of stress. The stress in the film was increased with increasing of annealing temperatures from +1.598 GPa (400 °C) to +2.033 GPa (900 °C). Discontinuities observed in the samples annealed at 300 and 1000 °C may be due to the formations and deformations of lattice structure with the annealing.

It is well known that film deposited on largely lattice mismatched substrates exhibit high density of linear

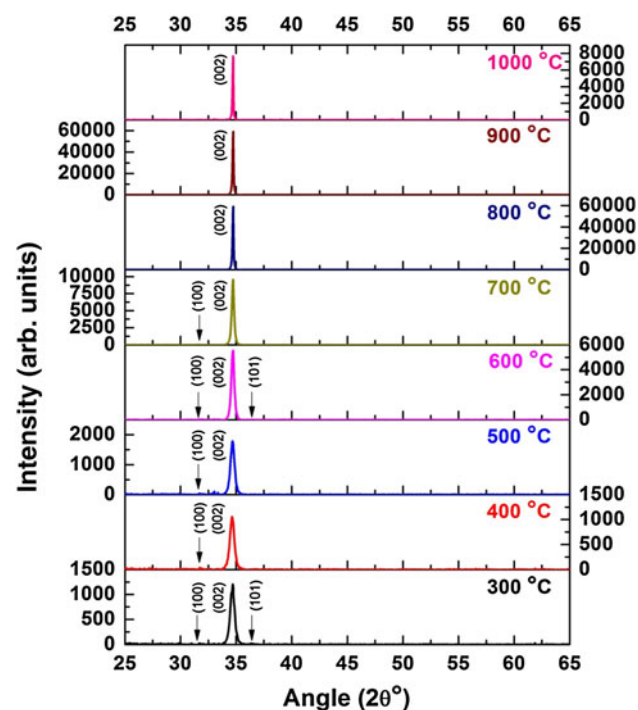


Fig. 1 XRD patterns of ZnO films annealed at various temperatures

defects. These dislocations are possible to characterize by broadening of FWHM in rocking curves. Mostly two types of dislocations are found in ZnO crystal lattices, edge dislocation and screw dislocations, which lead to twist and tilt in lattice planes respectively. The total dislocation density in a lattice structure expressed as

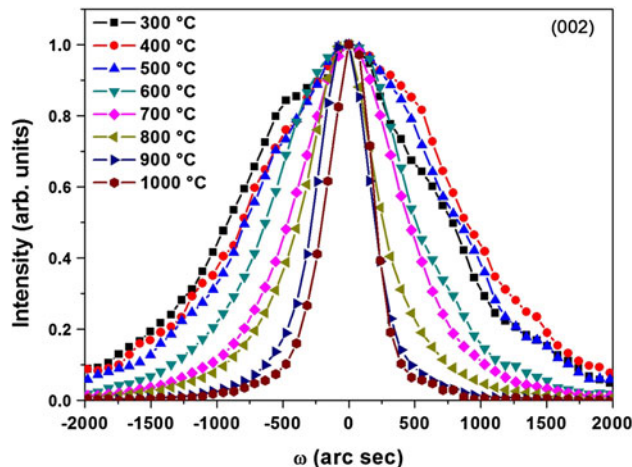


Fig. 2 Out-of-plane  $\omega$ -scan of (002) peak

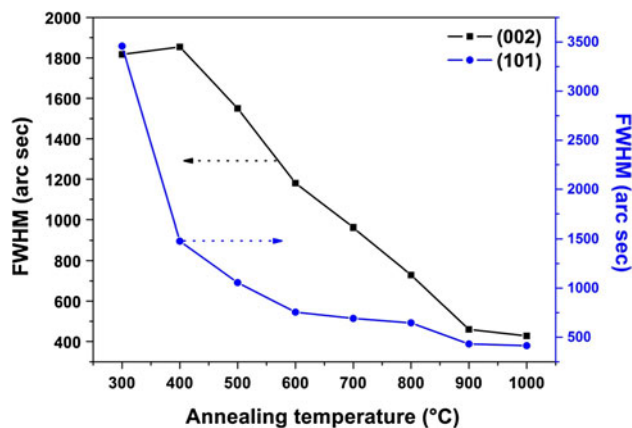


Fig. 3 Variation in FWHM of (002) and (101) peak as a function of annealing temperature

Table 1 Various physical parameters by sol–gel derived ZnO thin films as a function of annealing temperature

Sample	Peak position (2θ)	L. P. 'a' (Å)	L. P. 'c' (Å)	Stress (GPa)	Screw Dislocation density ( $\text{cm}^{-2}$ )	Grain size (nm)	Band gap (eV)
300 °C	34.699	3.257	5.166	+1.731	$1.67 \times 10^{10}$	14.2	3.38
400 °C	34.672	3.254	5.171	+1.554	$1.73 \times 10^{10}$	14.8	3.37
500 °C	34.695	3.255	5.170	+1.563	$1.21 \times 10^{10}$	18.6	3.36
600 °C	34.716	3.256	5.167	+1.705	$7.05 \times 10^9$	19.9	3.37
700 °C	34.718	3.254	5.164	+1.847	$4.69 \times 10^9$	21.2	3.38
800 °C	34.723	3.255	5.163	+1.883	$2.69 \times 10^9$	27.2	3.38
900 °C	34.723	3.255	5.161	+1.989	$1.07 \times 10^9$	31.9	3.38
1,000 °C	34.712	3.280	5.164	+1.817	$9.26 \times 10^8$	38.9	3.39

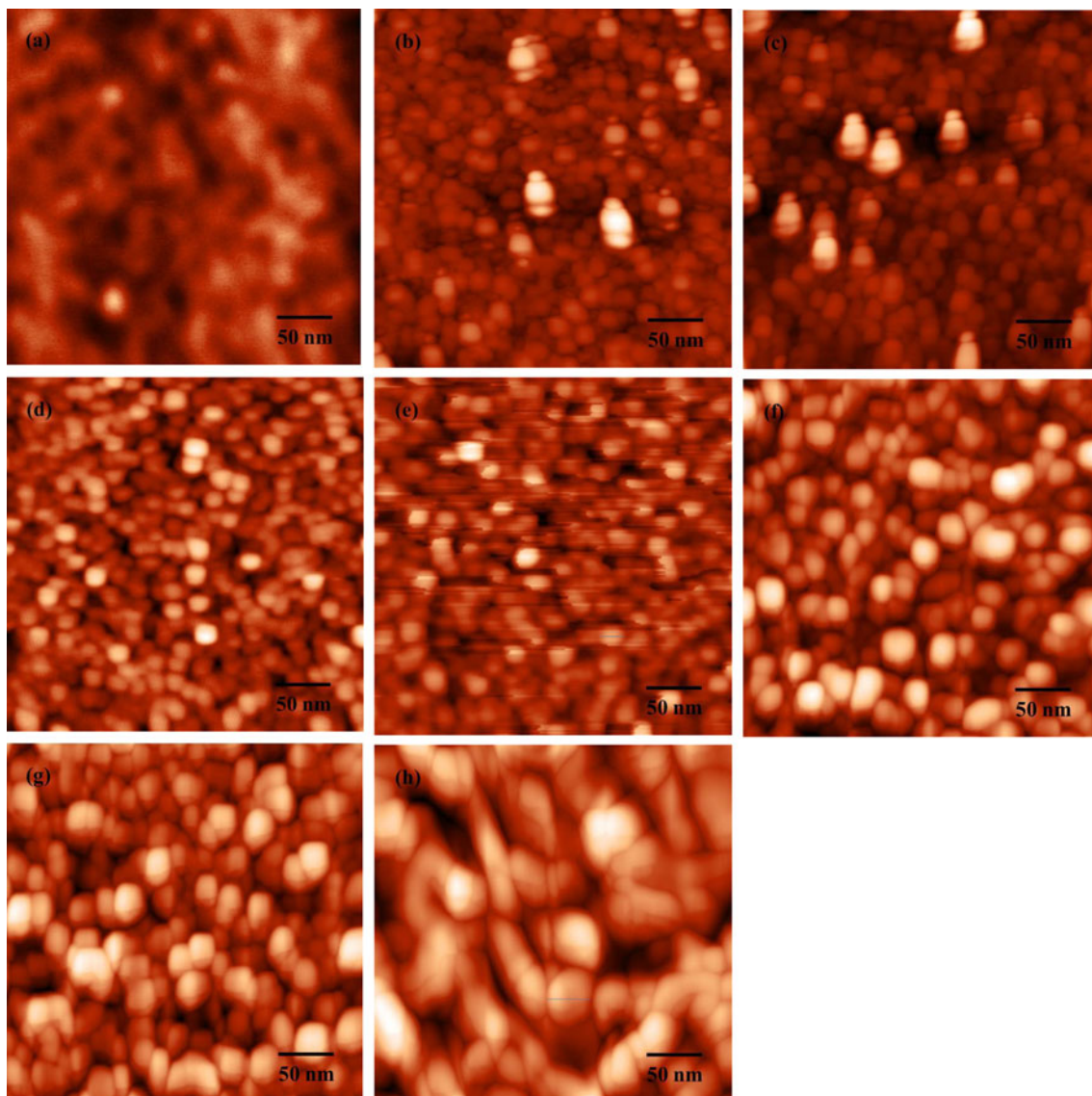
$$N_{dis} = N_{screw} + N_{edge} cm^{-2}$$

In a wurtzite crystal structure such as ZnO the screw dislocation with a burger vector  $\mathbf{b} = [001]$  results in a tilt of lattice planes, which in turn reflects itself in the FWHM of symmetric planes  $(00l)$  rocking curve in out-of-plane [21]. The edge dislocation with a burger vector  $\mathbf{b} = 1/3 [110]$  twist the lattice planes by azimuthal angel. This type of dislocations are only accessible either by  $\chi$ -scan of a reflection plane perpendicular to  $(00l)$  in transmission geometry, or by a  $\phi$ -scan of one of these planes in grazing incidence. Particularly, a component of the twist can be extracted from  $\omega$ -scan of asymmetrical  $(hkl; h \neq 0 \text{ and } l \neq 0)$  reflections measured in skew geometry [22].

Figure 2 shows out-of-plane  $\omega$ -scan of (002) peak. In contrast the FWHM of (002) peak decreased significantly with annealing. The FWHM corresponding to peak (002) and (101) are plotted against annealing temperature in Fig. 3. FWHM of (002) peak showed a linear decrease while the exponential reduction was observed for (101) peak. Screw dislocation density can be determined by following the expressions for wurtzite structures [23]

$$N_{screw} = \frac{\beta_{(ool)}^2}{9b_s^2}$$

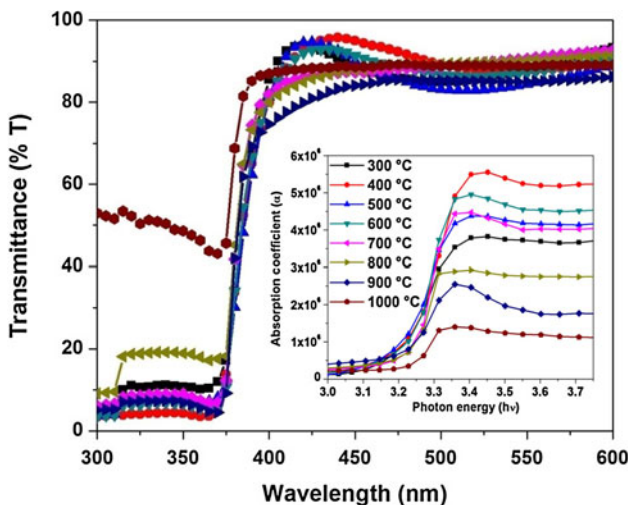
Where  $\beta$  is FWHM,  $b_s$  is burger vector lengths for [001] plane. Calculated values of screw dislocations are reproduced in Table 1.



**Fig. 4** AFM pictures for ZnO thin films recorded for different annealing temperatures: **a** 300 °C, **b** 400 °C, **c** 500 °C, **d** 600 °C, **e** 700 °C, **f** 800 °C, **g** 900 °C, **h** 1,000 °C

The surface morphology of the deposited ZnO thin films at different annealing temperatures was observed by atomic force microscopy as shown in Fig. 4. A strong influence of post annealing is observed on the grain sizes and microstructures of thin films, the grain size was

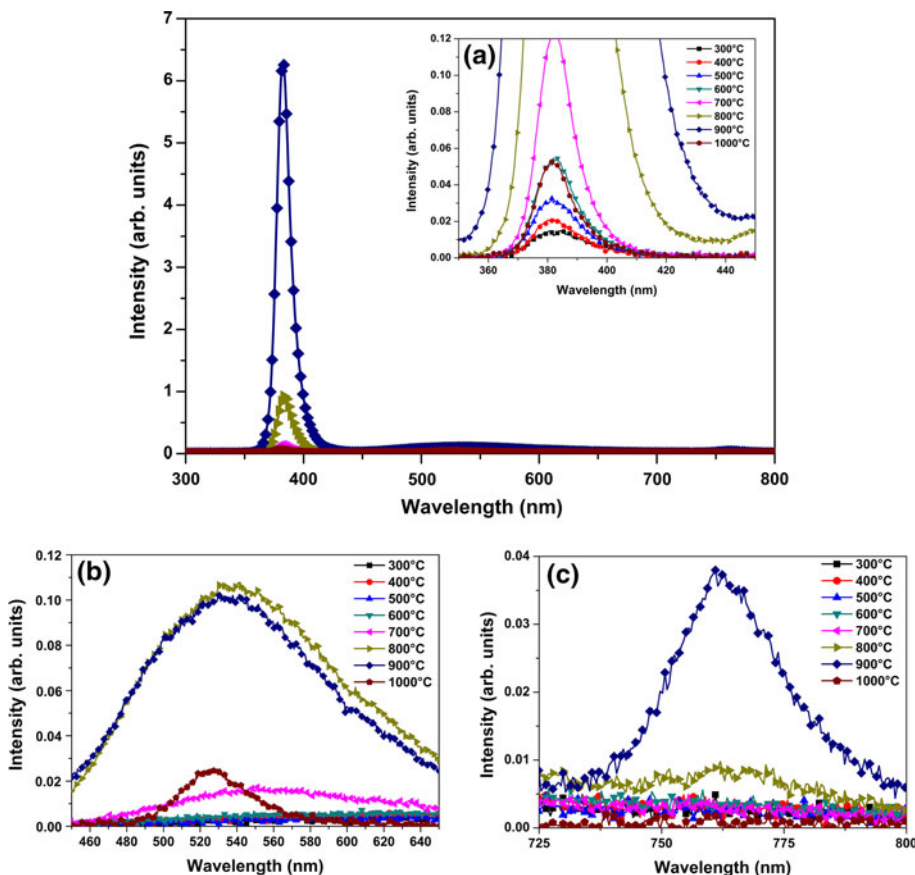
increased with post annealing temperature. It may be due to the integration of grains [24]. The grains are found to be in size of around 20 nm and spherical in shape for annealing temperatures up to 700 °C. For further annealing up to 900 °C the grains were noticed around 30 nm. The grain sizes are observed in ellipsoidal shapes for the sample annealed at 1000 °C. The grain sizes observed by AFM are in good agreement with the sizes calculated by XRD.



**Fig. 5** UV–Vis transmission spectra of ZnO thin films deposited on quartz glass. *Inset* showing variation in absorption coefficient of deposited films with annealing temperature

To determine the band gap, the films were deposited on the quartz glass. These films were examined by UV–Vis transmission spectroscopy. The transmission spectra of the deposited ZnO thin films at different annealing temperatures are shown in Fig. 5. The excitonic transitions were perceptibly observed in UV region. The band gap was not significantly affected by annealing, even though at lower annealing temperatures (400 and 500 °C) it slightly showed a red shift and the afterward band gap marginally enhanced. The band gap energy found around 3.37 eV. The sharp cut off of absorption edge was not clearly observed in the relating spectrum recorded for the sample annealed at 1,000 °C. It gives strength to the evidence that some kind of deformation in lattice structure took place may be due to the creation of SiO<sub>2</sub> at the interface of the substrate and/or breakage of the bonds in ZnO at 1,000 °C.

**Fig. 6** PL spectra of pure ZnO thin films measured at room temperature: **a** near band edge emission, **b** yellow–green emission associated to oxygen vacancies, **c** near infra-red emission observed at 800 and 900 °C (Color figure online)



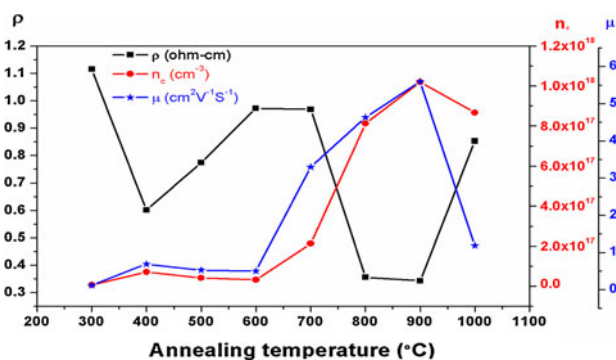


**Fig. 7** Variation in carrier concentration, Hall mobility and resistivity of ZnO films as a function of annealing temperature

**Table 2** Carrier concentration, Hall mobility and resistivity of ZnO films measured for the samples annealed at different temperatures

Sample	Carrier concentration (cm <sup>-3</sup> )	Hall mobility (cm <sup>2</sup> V <sup>-1</sup> s <sup>-1</sup> )	Resistivity (KΩ-cm)
300 °C	6.53 × 10 <sup>15</sup>	1.2	1.12
400 °C	7.17 × 10 <sup>16</sup>	6.9	0.60
500 °C	4.23 × 10 <sup>16</sup>	5.2	0.77
600 °C	3.23 × 10 <sup>16</sup>	5.0	0.97
700 °C	2.13 × 10 <sup>17</sup>	32.9	0.97
800 °C	8.13 × 10 <sup>17</sup>	46.3	0.36
900 °C	1.02 × 10 <sup>18</sup>	55.9	0.34
1,000 °C	8.67 × 10 <sup>17</sup>	11.8	0.85

The PL spectra of ZnO thin films annealed at 300 to 1,000 °C in the oxygen ambient observed at room temperature are shown in Fig. 6. The spectra exhibited strong and sharp near band edge emission (NBE) peak around 375 nm (3.36 eV). This characteristic peak is attributed to the radiative recombination of free excitons near band edge. It is evident from the spectra that the intensity of NBE peak was enhanced monotonically with increasing of annealing temperature. The intensity of this emission from the sample annealed at 900 °C is 300 times stronger as compared to sample annealed at 300 °C. It clearly indicated the significant influence of post annealing on the optical quality of ZnO thin films deposited by sol-gel route. The PL intensity reduced extensively for the sample annealed at 1,000 °C which may be due to poor optical quality of films at such a higher annealing temperature and confirm the pre postulate in XRD and UV-Vis spectroscopy results. A broad peak with comparatively very low intensity observed around 550 nm for the samples annealed at 700–900 °C. It is well accepted that this visible yellow-green emission is corresponding to transition between the conduction band and defect level created by oxygen vacancies ( $V_o^0$ ) [25]. So, higher annealing temperature

(≥700 °C) is responsible to create more defects in ZnO thin films. It is possibly due to evaporation of oxygen and/or breaking of bonds at such higher annealing temperatures and/or oxygen extracted by Si to be oxidized at interface [26, 27]. An infra-red emission with minute intensity was observed only in the sample heat treated at 800 and 900 °C. This emission could be related to  $V_o^{2+}$  (1.70 eV) defect levels as predicted by Kohan et al. [28].

The electrical resistivity of ZnO thin films was measured in Van der Pauw configuration; the variations in resistivity, carrier concentration and hall mobility of samples as a function of annealing temperature are plotted in Fig. 7. Initially the resistivity increased from 0.60 to 0.97 KΩ-cm as annealing temperature varied from 400 to 600 °C. The samples were annealed in oxygen ambient that concede good oxygen stoichiometry in thin films consequently be a reason of enhancement in the resistivity. The resistivity of ZnO samples is found in the range of as observed by Chu et al. [29] and Malek et al. [30]. Thereafter, as the annealing temperature further enhanced from 700 to 900 °C, it is found that the resistivity decreased from 0.97 to 0.34 KΩ-cm. It may be due to creation point defects as discussed and observed in PL measurements [26]. The uneven values of resistivity noticed for samples annealed at 300 and 1,000 °C possibly due to lattice formation (amorphous) and deformation, it implies some kind of discontinuity in the films and/or disorder in lattice. Hall measurement revealed that all the films are determined to n-type conductivity. Carrier concentration and mobility found in the range of  $n_c = 6.53 \times 10^{15}$  to  $1.02 \times 10^{18}$  cm<sup>-3</sup> and  $\mu = 1.2$ –55.9 cm<sup>2</sup>/Vs. Carrier concentrations was increased significantly in the samples as annealed from 700 to 900 °C, resulting from the increase in the number of possible donor levels ( $V_o/Zn_i$ ). The Scattering phenomenon such as lattice scattering and grain boundary scattering is reduced as the dislocations in the lattice decreased and the crystallinity of samples improved with annealing which lead to improve in hall mobility. The observed and calculated values of resistivity, carrier concentration and hall mobility are displayed in Table 2.

## 4 Conclusions

ZnO thin films were deposited successfully on p-Si (100) and quartz glass substrates by sol-gel spin coating method. Thin films were annealed at different temperatures to obtain a good quality ZnO sample. It is found that the average grain sizes, stress and optical luminescence enhanced with annealing. The band gap did not show any significant change with annealing and it was observed around 3.37 eV. Dislocations in the sol-gel derived ZnO

films were decreased with annealing. However, it is observed from photoluminescence spectra that at higher annealing temperatures ( $>700\text{ }^{\circ}\text{C}$ ) the point defects were increased. It is concluded from the detailed investigations for sol–gel derived ZnO thin films  $500\text{ to }700\text{ }^{\circ}\text{C}$  is the suitable temperature window for post annealing treatment.

**Acknowledgments** The authors wish to thank all the members of Hybrid Microcircuits group, CEERI, Pilani and Department of Electronic Science, K.U.K. for their technical support. The authors are extremely thankful to Dr. Chandra Shekhar, Director, CEERI, Pilani for his permission to utilize the facilities in his institution. One of authors Amanpal Singh is also thankful to Council of Scientific and Industrial Research (CSIR), India for award of senior research fellowship. This work was financially supported by the Department of Science and Technology, Ministry of Science, India, under the project number SR/S3/EECE/043/2007.

## References

- N.F. Hamedani, A.R. Mahjoub, A.A. Khodadadi, Y. Mortazavi, *Sens. Actuators B* **156**, 737 (2011)
- A. Jain, P. Sagar, R.M. Mehra, *Solid State Electron.* **50**, 1420 (2006)
- S.H. Lee, K.J. Byeon, H. Park, J.Y. Cho, K.Y. Yang, H. Lee, *Microelectron. Eng.* **88**, 3278 (2011)
- J.Y. Lee, J.H. Lee, H.S. Kim, C.H. Lee, H.S. Ahn, H.K. Cho, Y.Y. Kim, B.H. Kong, H.S. Lee, *Thin Solid Films* **517**, 5157 (2009)
- A. Mitra, R.K. Thareja, V. Ganesan, A. Gupta, P.K. Sahoo, V.N. Kulkarni, *Appl. Surf. Sci.* **174**, 232 (2001)
- K.W. Liu, D.Z. Shen, C.X. Shan, J.Y. Zhang, D.Y. Jiang, Y.M. Zhao, B. Yao, D.X. Zhao, *J. Phys. D Appl. Phys.* **41**, 125104 (2008)
- L. Cao, L. Zhu, J. Jiang, R. Zhao, Z. Ye, B. Zhao, *Sol. Energy Mater. Sol. Cells* **95**, 894 (2011)
- C.K. To, B. Yang, S.C. Su, C.C. Ling, C.D. Beling, S.J. Fung, *J. Appl. Phys.* **110**, 113521 (2011)
- S. Ghosh, A. Sarkar, S. Bhattacharya, S. Chaudhuri, A.K. Pal, *J. Cryst. Growth* **108**, 534 (1991)
- K. Shi, P.F. Zhang, H.Y. Wei, C.M. Jiao, P. Jin, X.L. Liu, S.Y. Yang, Q.S. Zhu, Z.G. Wang, *J. Appl. Phys.* **110**, 113509 (2011)
- S. Sadovef, S. Blumstengel, J. Cui, J. Puls, S. Rogaschewski, P. Schafer, F. Henneberger, *Appl. Phys. Lett.* **89**, 201907 (2006)
- A. Aksoy, Y. Caglar, S. Ilcan, M. Caglar, *J. Alloy. Compound.* **512**, 171 (2012)
- C.-H. Choi, S.-H. Kim, *J. Cryst. Growth* **283**, 170 (2005)
- F.K. Shan, G.X. Liu, B.C. Shin, W.J. Lee, *J. Korean Phys. Soc.* **54**, 916 (2009)
- A. Singh, D. Kumar, P.K. Khanna, A. Kumar, M. Kumar, M. Kumar, *Thin Solids Films* **519**, 5826 (2011)
- N. Fujimura, T. Nishihara, S. Goto, J. Xu, T. Ito, *J. Cryst. Growth* **130**, 269 (1993)
- C. Suryanaryana, M.G. Norton, *X-Ray Diffraction—A Practical Approach* (Plenum Press, New York, 1998)
- J. Karamdel, C.F. Dee, B.Y. Majlis, *SainsMalaysiana* **40**, 209 (2011)
- A. Singh, D. Kumar, P.K. Khanna, B.C. Joshi, M. Kumar, *Appl. Sur. Sci.* **258**, 1881 (2011)
- R. Cebulla, R. Wendt, K. Ellmer, *J. Appl. Phys.* **83**, 1087 (1998)
- Z. Vashaei, T. Minegishi, H. Suzuki, M.W. Cho, T. Yao, *J. Phys. Chem. Solids* **69**, 497 (2008)
- L. Wang, Y. Pu, W. Fang, J. Dai, C. Zheng, C. Mo, C. Xiong, F. Jiang, *Thin Solid Films* **491**, 323 (2005)
- M.K. Ozturk, Y. Hongbo, B. Sarikavak, S. Korack, S. Ozcelik, E. Ozbay, *J. Mater. Sci. Mater. Electron.* **21**, 85 (2010)
- C. Lee, J.H. Kim, S.K. Shin, *J. Korean Phys. Soc.* **53**, 3021 (2008)
- S.A. Studenikin, N. Golego, M. Cocivera, *J. Appl. Phys.* **84**, 2287 (1998)
- P. Sagar, P.K. Shishodia, R.M. Mehra, H. Okada, A. Wakahara, A. Yoshida, *J. Lumin.* **126**, 800 (2007)
- K. Vanheusden, W.L. Warren, C.H. Seager, D.R. Tallant, J.A. Voigt, B.E. Gnade, *J. Appl. Phys.* **79**, 7983 (1996)
- A.F. Kohan, G. Ceder, D. Morgan, *Phys. Rev. B* **61**, 15019 (2000)
- D. Chu, T. Hamada, K. Kato, Y. Masuda, *Phys. Status Solid A* **206**, 718 (2009)
- M.F. Malek, N. Zakaria, M.Z. Sahdan, M.H. Mamat, Z. Khusaimi, M. Rusop, *International Conference on Electronic Devices, Systems and Applications (ICEDSA, 2010)* p. 384. [http://ieeexplore.ieee.org/xpl/login.jsp?tp=&arnumber=5503037&url=http%3A%2F%2Fieeexplore.ieee.org%2Fxppls%2Fabs\\_all.jsp%3Farnumber%3D5503037](http://ieeexplore.ieee.org/xpl/login.jsp?tp=&arnumber=5503037&url=http%3A%2F%2Fieeexplore.ieee.org%2Fxppls%2Fabs_all.jsp%3Farnumber%3D5503037)